Available online at www.sciencedirect.com
SCIENCE DIRECT®
Journal of Solid State Chemistry 177 (2004) 1252–1257
JOURNAL OF SOLID STATE CHEMISTRY
http://elsevier.com/locate/jssc

The first metal phosphate incorporating isonicotinate ligand: synthesis, crystal structure, and solid-state NMR spectroscopy of $Zn(HINT)(HPO_4)$

Chih-Min Wang,[a] Shiuan-Ting Chuang,[a] Ya-Lan Chuang,[a] Hsien-Ming Kao,[a] and Kwang-Hwa Lii[a,b,*]

[a] *Department of Chemistry, National Central University, Chungli 320, Taiwan, ROC*
[b] *Institute of Chemistry, Academia Sinica, Nankang, Taipei 115, Taiwan, ROC*

Received 20 August 2003; received in revised form 20 October 2003; accepted 26 October 2003

Abstract

The first metal phosphate incorporating isonicotinate ligand, $Zn(HINT)(HPO_4)$, was hydrothermally synthesized and characterized by single-crystal X-ray diffraction and solid-state NMR spectroscopy. This compound crystallizes in the monoclinic space group $P2_1/c$ with cell parameters $a = 20.5643(8)$ Å, $b = 8.5169(4)$ Å, $c = 10.3928(4)$ Å, $\beta = 97.466(1)^\circ$, and $Z = 8$. The structure consists of 2D neutral sheets of zinc hydrogen phosphate with the dipolar isonicotinate ligand being coordinated to zinc as a pendent group. Adjacent sheets are connected by hydrogen bonding. The ^1H magic angle spinning NMR spectrum exhibits three resonances at 15.5, 8.1, and 4.8 ppm with an intensity ratio close to 1:4:1, corresponding to two different types of protons in isonicotinate ligand and one type of protons in hydrogen phosphate groups. The peak at 15.5 ppm can be assigned to the proton bonded to the pyridine nitrogen atom, which confirms the presence of $^+HNC_5H_4COO^-$.

Keywords: Zinc phosphate; Isonicotinate; Crystal structure; Solid-state NMR

1. Introduction

The synthesis of open-framework metal phosphates has been a subject of intense research owing to their interesting structural chemistry and potential applications as adsorbents, catalysts, and ion-exchange media. A large number of these materials have been synthesized in the presence of organic amines as structure-directing agents [1–3]. Recently, many research activities have focused on the synthesis of organic–inorganic hybrid compounds by incorporating organic ligands such as the anionic oxalate or neutral 4,4′-bipyridine in the structures of metal phosphates. The underlying idea is to combine the robustness of inorganic phosphate frameworks with the versatility and chemical flexibility of organic ligands. A large number of oxalate-phosphates and 4,4′-bpy-phosphates of transition metals and group 13 elements have been reported [4,5]. We have recently become interested in the synthesis of metal phosphates with the multifunctional organic ligand isonicotinate (abbreviated as INT) (4-pyridinecarboxylate) in which both neutral N-donor and anionic O-donor groups are present, because several coordination polymers based on INT ligand have shown interesting physical properties and structural chemistry [6–11]. For example, $Zn(INT)_2$ is a potentially useful NLO material with high thermal stability [6]. $\{[Cu_2(INT)_4 \cdot 3H_2O]\ [Cu_2(INT)_4 \cdot 2H_2O]\} \cdot 3H_2O$ has an interpenetrating structure with two covalently bonded open frameworks of different dimensionality [9]. Here, we report the synthesis and structural characterization of the first example of metal phosphate incorporating isonicotinate ligand: $Zn(HINT)(HPO_4)$.

2. Experimental

2.1. Synthesis and initial characterization

The hydrothermal reactions were carried out in Teflon-lined stainless steel Parr acid digestion bombs

*Corresponding author. Institute of Chemistry, Academia Sinica, Nankang, Taipei 115, Taiwan, ROC. Fax: +886-3-422-7664.
E-mail address: liikh@cc.ncu.edu.tw (K.-H. Lii).

0022-4596/$ - see front matter © 2003 Elsevier Inc. All rights reserved.
doi:10.1016/j.jssc.2003.10.033

with an internal volume of 23 mL. All chemicals were purchased from Aldrich. Reaction of ZnO (1 mmol), isonicotinic acid (1 mmol), H_3PO_4 (10 mmol), H_2O (7 mL), and CH_3CN (3 mL) at 120°C for 3 days produced colorless tablet crystals of Zn(HINT)(HPO_4), **1**. The pH of reaction mixture after hydrothermal reaction was 2.7. The product was filtered, washed with water, rinsed with ethanol, and dried in a desiccator. Powder X-ray diffraction pattern of the bulk product is in good agreement with the calculated pattern based on the results from single-crystal X-ray diffraction (Fig. 1). The yield was 48% based on Zn. Energy-dispersive X-ray fluorescence spectroscopy of several colorless crystals confirms the presence of Zn and P. Elemental analysis results of the bulk product are consistent with the stoichiometry of **1**. Anal. found: C, 25.13%; H, 2.19%; N, 4.59%. Calcd: C, 25.33%; H, 2.13%; N, 4.92%. Thermogravimetric analysis (TGA), using a Perkin Elmer TGA7 thermal analyzer, was performed on a powder sample in flowing oxygen atmosphere in the temperature range of 40–900°C with a heating rate of 10°C min^{-1}. The TGA curve showed weight loss in several overlapping steps between 300°C and 600°C (Fig. 2). The final decomposition product was $Zn_2P_2O_7$ (JCPDS 43-0488) as indicated by powder X-ray diffraction. The observed total weight loss between 40°C and 900°C was 46.43% which is in good agreement with that calculated for the loss of one molecule of isonicotinic acid and a half molecule of H_2O (46.45%).

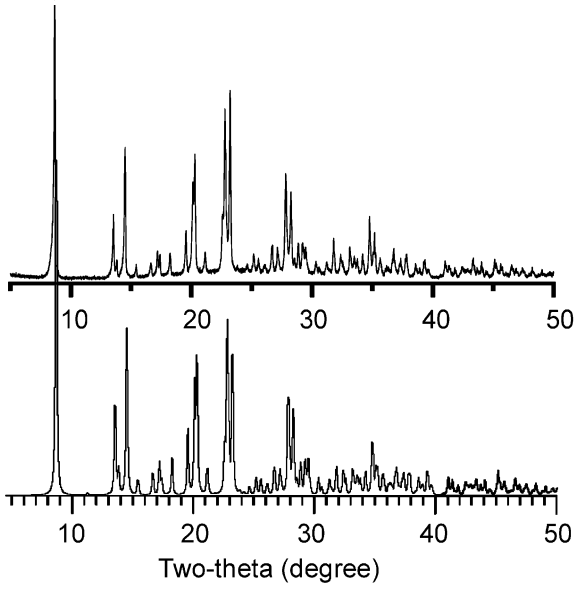

Fig. 1. Experimental X-ray powder pattern (top) and simulated powder pattern based on the results from single-crystal X-ray diffraction (bottom) for **1**.

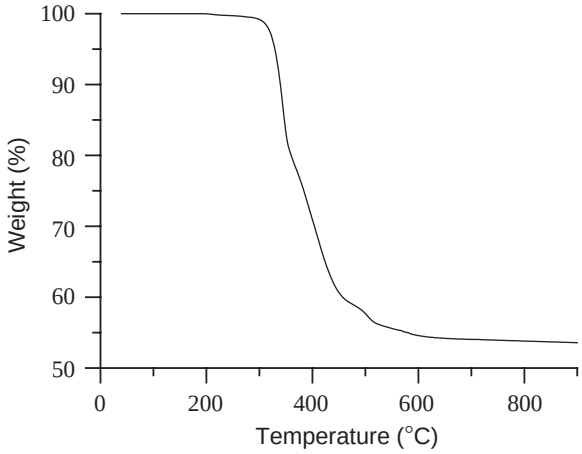

Fig. 2. TGA of **1** in flowing oxygen at 10°C min^{-1}.

2.2. Single-crystal X-ray diffraction

A suitable crystal of **1** with dimensions $0.34 \times 0.19 \times 0.12\,mm^3$ was selected for indexing and intensity data collection on a Siemens SMART CCD diffractometer equipped with a normal focus, 3-kW sealed tube X-ray source. Intensity data were collected at room temperature in 1271 frames with ω scans (width 0.30° per frame). Empirical absorption corrections based on symmetry equivalents were applied. The structure was solved by direct methods and difference Fourier syntheses. Bond-valence calculation results indicate that O(1) and O(5) are hydroxo oxygen atoms [12]. The H atoms in the hydroxo groups were located in difference Fourier maps. The H atoms, which are bonded to C atoms, were positioned geometrically and refined using a riding model. The H atoms bonded to N atoms were also located. The final cycles of least-squares refinement included atomic coordinates and anisotropic thermal parameters for all nonhydrogen atoms and isotropic thermal parameters for hydroxo and pyridinium H atoms. The final difference Fourier maps were flat ($\Delta\rho_{max,\,min} = 0.40,\ -0.40\,e\,Å^{-3}$). All calculations were performed using the SHELXTL Version 5.1 software package [13]. CIF file for **1** has been deposited with the Cambridge Crystallographic Data Centre as supplementary publication no. CCDC-216559.

2.3. Solid-state NMR measurements

All NMR spectra were acquired on a Bruker AVANCE-400 spectrometer, operating at 400.1 and 161.9 MHz for ^1H and ^{31}P nuclei, respectively. A Bruker probe equipped with 4 mm rotors was used. ^1H magic angle spinning (MAS) NMR spectra were recorded at a spinning speed of 12 kHz. The 90° pulse lengths of ^1H and ^{31}P were 2.0 and 4.0 μs, respectively. Recycle delays of 3 and 50 s were used for ^1H and ^{31}P NMR. The chemical shifts were externally referenced to

tetramethylsilane for ^{1}H NMR and 85% $H_3PO_{4(aq)}$ for ^{31}P NMR.

3. Results and discussion

3.1. Description of the structure

The crystal data and structure refinement parameters are given in Table 1, atomic coordinates and thermal parameters in Table 2, and selected bond lengths in Table 3. All atoms are at general positions. The asymmetric unit contains two Zn^{2+} cations, two neutral HINT ligands, and two HPO_4^{2-} anions. Fig. 3 shows the coordination environments of two Zn atoms and atom labeling scheme. Each Zn is tetrahedrally coordinated by three phosphate groups and one carboxylate group of an HINT unit in a monodentate fashion. Each phosphorus atom is bonded to three Zn atoms through three oxygen atoms with the fourth coordination site being a terminal P–OH group. Both HINT ligands are dipolar ions, namely, the carboxylate group loses a proton, giving a carboxylate ion, and the pyridine nitrogen is protonated to a pyridinium ion. The pyridyl ring and carboxylate group are slightly twisted at an angle of 11.9° and 2.1° for the HINT ligands which coordinate to Zn(1) and Zn(2), respectively.

The structure consists of two-dimensional neutral sheets of Zn(HINT)(HPO_4) in the *bc* plane (Fig. 4). There are two sheets per unit cell length along the *a*-axis. Each sheet, shown in Fig. 5, is constructed from strictly alternating ZnO_4 and HPO_4 tetrahedra sharing vertices. The covalent connectivity in each layer produces four-membered $\{Zn_2P_2\}$ rings and eight-membered $\{Zn_4P_4\}$ rings, which fuse to propagate the network structure. The HINT ligands coordinate to Zn atoms and extend away from the layer into the interlamellar region as pendent groups. The HINT ligand which coordinates to Zn(1) alternates along the *b*-axis with the HINT ligand to Zn(2) belonging to an adjacent ZnPO layer. Neighboring HINT ligands from adjacent layers have a structure of offset nonparallel stacking and are separated by 4.26 Å; hence, intermolecular aromatic interaction is weak. There are hydrogen bonds between adjacent layers as indicated by the short H(1N)···O(7) distance of 1.77 Å and N(1)–H(1N)–O(7) bond angle of 171°. The other pyridinium hydrogen, H(2N), is not involved in any hydrogen bonding. The HPO_4^{2-} groups form hydrogen bonds with the carboxylate groups within the same layer.

Table 1
Crystallographic data for Zn(HINT)(HPO_4)

Formula	$C_6H_6NO_6PZn$
M	284.45
Crystal system	Monoclinic
Space group	$P2_1/c$ (No. 14)
a (Å)	20.5643(8)
b (Å)	8.5169(4)
c Å)	10.3928(4)
β (deg)	97.466(1)
V (Å^3)	1804.8(2)
Z	8
T (K)	296
λ(Mo*K*α) (Å)	0.71073
D_{calc} (g cm^{-3})	2.094
μ(Mo*K*α) (cm^{-1})	29.1
Measured reflections	13023
Unique reflections (R_{int})	4463 (0.0247)
Observed reflections [$I > 2\sigma(I)$]	3867
R_1[a]	0.0236
wR_2[b]	0.0646

[a] $R_1 = \sum||F_o| - |F_c||\sum|F_o|$.
[b] $wR_2 = \sum\{[w(F_o^2 - F_c^2)^2]/\sum[w(F_o^2)^2]\}^{1/2}$, $w = 1/[\sigma^2(F_o^2) + (aP)^2 + bP]$, $P = [\mathrm{Max}(F_o, 0) + 2(F_c)^2]/3$, where $a = 0.0397$ and $b = 0$.

Table 2
Atomic coordinates and thermal parameters (Å^2) for Zn(HINT)(HPO_4)[a]

Atom	*x*	*y*	*z*	U_{eq}[b]
Zn(1)	−0.43980(1)	0.08150(2)	0.34836(2)	0.02095(7)
Zn(2)	0.06462(1)	0.19138(2)	−0.07297(2)	0.02110(7)
P(1)	−0.52187(2)	−0.20962(5)	0.39102(4)	0.0199(1)
P(2)	0.02406(2)	0.09350(5)	0.18275(4)	0.0197(1)
O(1)	−0.57829(7)	−0.0939(2)	0.3330(1)	0.0319(3)
O(2)	−0.45852(6)	−0.1392(2)	0.3588(1)	0.0279(3)
O(3)	−0.53265(7)	−0.3711(2)	0.3312(1)	0.0288(3)
O(4)	−0.52315(6)	−0.2250(2)	0.5373(1)	0.0251(3)
O(5)	0.07952(7)	−0.0354(2)	0.1897(1)	0.0289(3)
O(6)	0.04219(7)	0.2294(2)	0.1004(1)	0.0264(3)
O(7)	0.01955(6)	0.1451(2)	0.3227(1)	0.0241(3)
O(8)	−0.04053(6)	0.0177(2)	0.1308(1)	0.0268(3)
O(9)	−0.34343(7)	0.0950(2)	0.3654(2)	0.0429(4)
O(10)	−0.30949(8)	0.1220(2)	0.5780(2)	0.0509(4)
O(11)	0.15946(7)	0.2058(2)	−0.0772(2)	0.0357(3)
O(12)	0.18622(9)	0.0327(2)	0.0817(2)	0.0673(6)
N(1)	−0.10476(8)	0.1105(2)	0.3794(2)	0.0308(4)
N(2)	0.39563(9)	0.1352(2)	−0.0812(2)	0.0381(4)
C(1)	−0.3006(1)	0.1081(2)	0.4636(2)	0.0306(4)
C(2)	−0.23053(9)	0.1093(2)	0.4332(2)	0.0262(4)
C(3)	−0.2173(1)	0.1256(3)	0.3060(2)	0.0333(4)
C(4)	−0.1535(1)	0.1238(3)	0.2813(2)	0.0342(5)
C(5)	−0.1157(1)	0.0971(2)	0.5021(2)	0.0341(5)
C(6)	−0.1785(1)	0.0940(2)	0.5316(2)	0.0326(4)
C(7)	0.1991(1)	0.1215(3)	−0.0044(2)	0.0336(4)
C(8)	0.26985(9)	0.1296(2)	−0.0308(2)	0.0289(4)
C(9)	0.2879(1)	0.2254(3)	−0.1287(2)	0.0375(5)
C(10)	0.3521(1)	0.2261(3)	−0.1523(2)	0.0410(5)
C(11)	0.3807(1)	0.0429(3)	0.0138(2)	0.0388(5)
C(12)	0.3172(1)	0.0387(3)	0.0408(2)	0.0352(5)
H(1O)	−0.618(2)	−0.108(4)	0.365(3)	0.09(1)
H(5O)	0.107(1)	−0.019(3)	0.152(2)	0.043(8)
H(1N)	−0.061(2)	0.112(3)	0.356(3)	0.08(1)
H(2N)	0.434(1)	0.135(3)	−0.094(2)	0.047(7)

[a] The H atoms which are bonded to C atoms are given in supplementary materials.
[b] U_{eq} is defined as one-third of the trace of the orthogonalized U_{ij} tensor.

Table 3
Bond lengths (Å) for $Zn(HINT)(HPO_4)$[a]

Zn(1)–O(2)	1.924(1)	Zn(1)–O(3)	1.921(1)
Zn(1)–O(4)	1.929(1)	Zn(1)–O(9)	1.970(1)
Zn(2)–O(6)	1.944(1)	Zn(2)–O(7)	1.927(1)
Zn(2)–O(8)	1.924(1)	Zn(2)–O(11)	1.960(1)
P(1)–O(1)	1.581(1)	P(1)–O(2)	1.511(1)
P(1)–O(3)	1.514(1)	P(1)–O(4)	1.530(1)
P(2)–O(5)	1.578(1)	P(2)–O(6)	1.515(1)
P(2)–O(7)	1.534(1)	P(2)–O(8)	1.512(1)
O(1)–H(1O)	0.93(3)	O(5)–H(5O)	0.74(3)
C(1)–O(9)	1.262(2)	C(1)–O(10)	1.231(2)
C(1)–C(2)	1.516(3)	C(2)–C(3)	1.392(3)
C(2)–C(6)	1.387(3)	C(3)–C(4)	1.368(3)
C(5)–C(6)	1.365(3)	N(1)–C(4)	1.339(3)
N(1)–C(5)	1.328(3)	N(1)–H(1N)	0.95(3)
C(7)–O(11)	1.262(2)	C(7)–O(12)	1.227(3)
C(8)–C(9)	1.392(3)	C(8)–C(12)	1.382(3)
C(9)–C(10)	1.373(3)	C(11)–C(12)	1.371(3)
N(2)–C(10)	1.332(3)	N(2)–C(11)	1.329(3)
N(2)–H(2N)	0.82(3)		

[a] The C–H bond lengths are 0.93 Å.

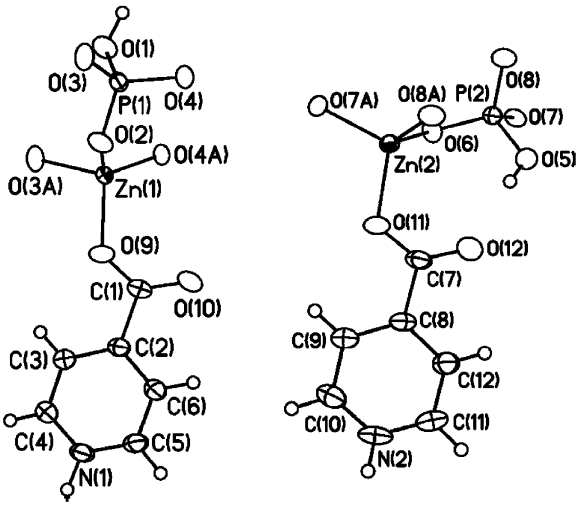

Fig. 3. The coordination environments of Zn atoms in the structure of **1** showing atom labeling scheme. Thermal ellipsoids are shown at 50% probability. Small open circles are H atoms.

We note that the structure of **1** is closely related to those of the zinc chlorophosphate $[C_6NH_{14}][ZnCl(HPO_4)]$ and the tin(II) phosphate $[C_3N_2H_{12}]_{0.5}[SnPO_4]$ [14,15]. The former consists of macroanionic inorganic layers of zincophosphate with the organic cations between the layers. Each layer is built up from ZnO_3Cl and HPO_4 tetrahedra, linked by corners in the same way as that in **1** to form four- and eight-membered apertures. The chlorine atoms are directed into the interlamellar region. Similar positioning is also observed for the isonicotinate ligand in **1**. $[C_3N_2H_{12}]_{0.5}[SnPO_4]$ has a similar layer structure. The stereo-active lone pair of electrons of Sn(II) provides the fourth vertex needed for the $\varphi - 4t$ tetrahedron, which occupies an identical position to that of the chlorine atom in the zinc chlorophosphate.

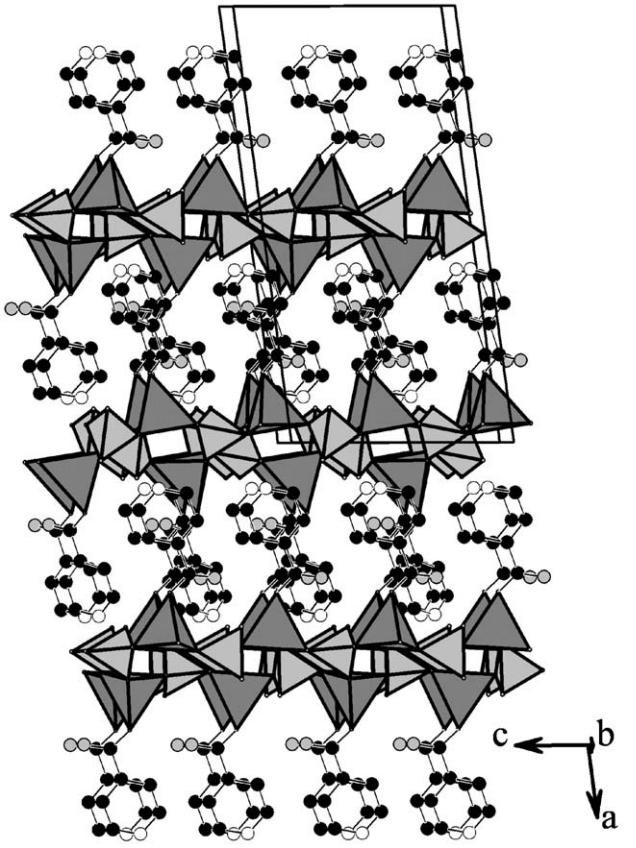

Fig. 4. Structure of **1** viewed along the *b*-axis. The dark and light gray polyhedra are ZnO_4 and HPO_4 tetrahedra, respectively. Black circles, C atoms; gray circles, O atoms; open circles, N atoms. H atoms are not shown.

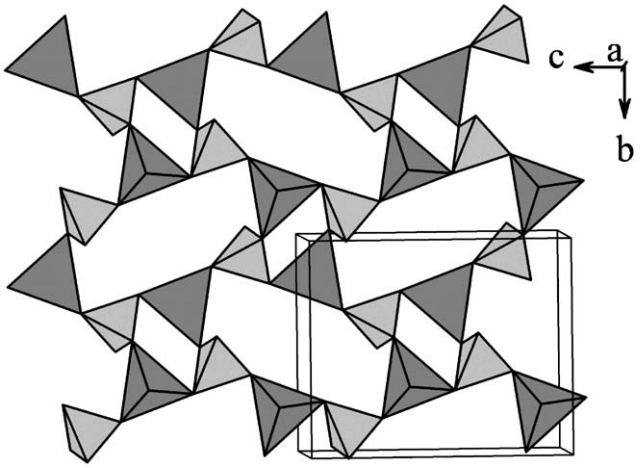

Fig. 5. Section of a zinc phosphate layer in **1** viewed along the *a* axis.

3.2. ^1H MAS NMR

Fig. 6 shows the ^1H MAS NMR spectrum of **1**, along with the assignments to specified protons as indicated in

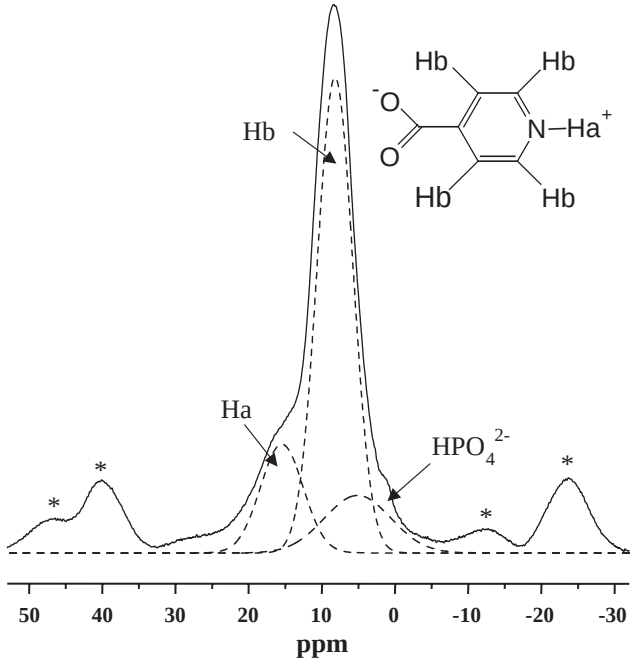

Fig. 6. ^{1}H MAS NMR spectrum of **1** acquired at a spinning speed of 12 kHz. The spectrum was deconvoluted using three peaks in an intensity ratio close to 1:4:1 for two different types of protons in dipolar isonicotinate ligands and one type of protons in hydrogen phosphate groups, respectively, as shown in dashed lines.

the inset of the figure. Three major resonances are observed at 15.5, 8.1, and 4.8 ppm. The resonance at 8.1 ppm is assigned to the protons in the aromatic ring. The peak at 15.5 ppm is indicated from its downfield character and a comparison with the ^{1}H MAS NMR spectrum of $[(VO_2)_2(4,4'\text{-bpy})_{0.5}(4,4'\text{-Hbpy})(PO_4)]\cdot H_2O$ to be assigned to the protons bonded to the pyridine nitrogen atoms [5(d)], which confirms the presence of dipolar $^{+}HNC_5H_4COO^{-}$ ligand. The resonance at 4.8 ppm is ascribed to the protons of the hydrogen phosphate groups. The ^{1}H NMR spectrum was deconvoluted using three peaks as shown in dashed lines in Fig. 6. The intensity ratio of the three resonances at 15.5, 8.1, and 4.8 ppm, obtained from the intensity sum of the isotropic peaks and their respective spinning sidebands, is equal to 1.0: 3.9: 0.9, which is in good agreement with the stoichiometry of **1** (1:4:1) as determined from X-ray diffraction. The ^{31}P MAS NMR spectrum exhibits two resonances at 6.8 and 5.0 ppm with nearly the same peak areas, which correspond to two distinct phosphate groups in the structure.

3.3. Concluding remarks

In summary, we have synthesized the first example in the metal-isonicotinate-phosphate system. The structure consists of $Zn(HPO_4)$ layers with the dipolar isonicotinate ligand being coordinated to zinc as a pendent group. The presence of $^{+}HNC_5H_4COO^{-}$ is confirmed by ^{1}H MAS NMR spectroscopy. Recent studies have shown that isonicotinate tends to bind metal centers with both pyridyl and carboxylate groups to form 3D coordination polymers, where carboxylate groups balance the metal charges. In the structure of **1** the HPO_4^{2-} group balances the metal charge and the isonicotinate ligand binds the metal center with the carboxylate group only. In order for isonicotinate to coordinate to metal centers with both the neutral and anionic groups, one may introduce a counter cation in the structure. Compounds with many possible compositions of anionic sub-lattice and different counter cations can be envisaged. Bimetallic compounds are also highly interesting. Further research to synthesize open-framework materials in the M/INT/PO system by including appropriate organic amine templates in their structures is in progress.

Acknowledgments

We thank the National Science Council for support, Ms. F.-L. Liao and Prof. S.-L. Wang at the National Tsing Hua University for X-ray data collection, and Ms. R.-R. Wu at National Cheng Kung University for NMR spectra measurements.

References

[1] R.C. Haushalter, L.A. Mundi, Chem. Mater. 4 (1992) 31 (and references therein).
[2] K.-H. Lii, Y.-F. Huang, V. Zima, C.-Y. Huang, H.-M. Lin, Y.-C. Jiang, F.-L. Liao, S.-L. Wang, Chem. Mater. 10 (1998) 2599 (and references therein).
[3] A.K. Cheetham, G. Férey, T. Loiseau, Angew. Chem. Int. Ed. 38 (1999) 3268 (and references therein).
[4] (a) H.-M. Lin, K.-H. Lii, Y.-C. Jiang, S.-L. Wang, Chem. Mater. 11 (1999) 519;
(b) C.-Y. Chen, P.P. Chu, K.-H. Lii, Chem. Commun. 16 (1999) 1473;
(c) Z.A.D. Lethbridge, P. Lightfoot, J. Solid State Chem. 143 (1999) 58;
(d) Z.A.D. Lethbridge, A.D. Hiller, R. Cywinske, P. Lightfoot, J. Chem. Soc. Dalton Trans. 10 (2000) 1595;
(e) A. Choudhury, S. Natarajan, C.N.R. Rao, J. Solid State Chem. 146 (1999) 538;
(f) A. Choudhury, S. Natarajan, C.N.R. Rao, Chem. Eur. J. 6 (2000) 1168;
(g) Y.-C. Jiang, S.-L. Wang, K.-H. Lii, N. Nguyen, A. Ducouret, Chem. Mater. 15 (2003) 1633 (and references therein).
[5] (a) K.-H. Lii, Y.-F. Huang, Inorg. Chem. 38 (1999) 1348;
(b) C.-Y. Chen, F.-R. Lo, H.-M. Kao, K.-H. Lii, Chem. Commun. 12 (2000) 1061;
(c) Y.-C. Jiang, Y.-C. Lai, S.-L. Wang, K.-H. Lii, Inorg. Chem. 40 (2001) 5320;
(d) L.-H. Huang, H.-M. Kao, K.-H. Lii, Inorg. Chem. 41 (2002) 2936;
(e) Z. Shi, S. Feng, S. Gao, L. Zhang, G. Yang, J. Hua, Angew. Chem. Int. Ed. 39 (2000) 2325;

(f) Z. Shi, S. Feng, L. Zhang, G. Yang, J. Hua, Chem. Mater. 12 (2000) 2930.
[6] O.R. Evans, R.-G. Xiong, Z. Wang, G.K. Wong, W. Lin, Angew. Chem. Int. Ed. 38 (1999) 536.
[7] L. Ma, O.R. Evans, B.M. Foxman, W. Lin, Inorg. Chem. 39 (1999) 5837.
[8] M.E. Chapman, P. Ayyappan, B.M. Foxman, G.T. Yee, W. Lin, Crystal Growth Des. 1 (2001) 159.
[9] J.Y. Lu, A.M. Babb, Chem. Commun. 9 (2001) 821.
[10] J.Y. Lu, A.M. Babb, Inorg. Chem. 40 (2001) 3261.
[11] J.Y. Lu, A.M. Babb, Chem. Commun. 13 (2002) 1340.
[12] I.D. Brown, D. Altermatt, Acta Crystallogr. B 41 (1985) 244.
[13] G.M. Sheldrick, SHELXTL Programs, Version 5.1; Bruker AXS GmbH, Karlsruhe, Germany, 1998.
[14] S. Neeraj, S. Natarajan, J. Mater. Chem. 10 (2000) 1171.
[15] S. Ayyappan, X. Bu, A.K. Cheetham, S. Natarajan, C.N.R. Rao, Chem. Commun. 20 (1998) 2181.